

SELF-CENTERING CONCRETE COUPLED WALL WITH FLAG-SHAPED HYSTERESIS DAMPING SYSTEM FOR SEISMIC PROTECTION OF BUILDING STRUCTURES

Luhur BUDI¹,

Abstract: Research showed that the concrete coupled wall is the outstanding seismic resisting systems for high-rise building structures which located in a high seismic region. In this system, the link beam provides coupling action between the beam and the adjacent wall panel, which significantly increases the wall system's lateral stiffness and reduce the footprint for the seismic resisting system. However, once the link beam is damaged due to a severe earthquake, it is difficult, costly, and time-consuming to be repaired, which results in business disruption and other financial loss. The low damage design concept is proposed to respond to this challenge. Its main objective is to design a structure that cannot only survive under a severe earthquake but also can be immediately occupied with negligible repair. In this way, business disruption and building demolition after an earthquake can be mitigated. As a low damage solution, the concrete coupled wall should provide a rocking mechanism at the wall base for providing free rotation and releasing bending moment demand. However, this rocking motion should be controlled by a set of damping devices that provide high lateral stiffness, damping, and self-centring behaviour. The RSFJ has recently been introduced and employed in the New Zealand construction industry. This technology can provide life safety and minimises earthquake damage so that the building can be reoccupied immediately with minimal business disruption. The flag-shaped hysteresis of the RSFJs provides an excellent energy dissipation and self-centring behaviour. This paper provides a robust step-by-step analysis and design procedure for engineers in practice and researchers for designing a structure with flag-shaped hysteresis damping systems. An eight-storey reinforced concrete building is designed using the forced-based design method, and its seismic performance is evaluated by non-linear static pushover and nonlinear dynamic time-history simulations. The results showed that this system can provide a high level of structural ductility while providing fully self-centring behaviour.

Introduction

The two deadly Canterbury earthquakes that occurred on February 22 and June 13, 2011, claimed hundreds of people's lives and damaged nearly a thousand buildings. Chancellor et al. (2014) noted that these earthquakes destroyed almost 1000 buildings in the central business district, which needed to be subsequently demolished due to their permanent damage after the earthquake. Djojo (2016) reported that during these earthquake series, the low ductility structures experienced minor damage while the high ductility building suffered severe deterioration. The Treasury New Zealand (2014) estimated that it costs about NZD\$40 billion nearly 20% of New Zealand's GDP, for reconstructing these infrastructures. This value did not consider the additional financial loss incurred with business downtime. Therefore, a resilient building structure which provides an excellent seismic performance and self-centring behaviour is necessarily needed.

Previous studies showed that the concrete coupled wall is one of the outstanding seismic resisting systems for high-rise building structures which located in a high seismic region. In this system, the link beam provides coupling action between the beam and the adjacent wall panel, which significantly increases the wall system's lateral stiffness and eventually reduces the footprint for the seismic resisting system. However, once the link beam is damaged due to a severe earthquake, it is difficult, costly, and time-consuming to be repaired, which results in business disruption and other financial loss. Therefore, many researchers attempted to add the flag-shaped hysteresis damping system (e.g., post-tensioning strands, shape memory alloy bars, metallic dampers, and friction dampers) to alleviate the damage in the beam. Nevertheless, these systems are lack of self-centring mechanism (i.e., each damping device requires an additional system), poor repairability, and need regular maintenance. Furthermore, the post-tensioned steel beam,

¹ Stationary Engineer, PT. Pertamina (Persero), Kota Dumai, Indonesia, luhur.budi@pertamina.com

when employed as a damper in the coupling beam, leads to complexities and difficulties during the construction stage.

To respond to the above challenges, Zarnani and Quenneville (2015) introduced a new technology, known as the Resilient Slip Friction Joint (RSFJ). It provides essential energy absorption and self-centering capability, and other excellent features, including secondary fuse activation, easy reparability, and free maintenance, to ensure life “safety” and “immediate occupancy” criteria post-earthquake. This research project proposed a concrete coupled wall structure using the RSFJ to produce an efficient and high-performance lateral load-resisting system.

The objective of this research is to provide a robust step by step analysis and design procedure for implementing RSFJ device in concrete coupled wall. This procedure will help engineer to select the appropriate design method and efficient damper size such that extra cost associated with inefficient sizing of the structure and the damper can be avoided. The basic equations and the hysteresis curve of the RSFJ are introduced. The specific configuration of the RSFJ will be proposed, and the procedure to design RSFJ specification will be developed. The effect of the RSFJ damping device in increasing the seismic performance of the building structure will be further investigated. Finally, the numerical modelling is developed, and its structural analysis result is verified.

Resilient Slip Friction Joint (RSFJ)

The RSFJ technology is a novel friction joint that provides energy absorption and self-centering behaviour in one compact package. The main component of the RSFJ comprises an elongated holes steel plate, metal cap plate, high strength bolts, and disc springs, as shown in Figure 1. In RSFJ, the restoring force comes from specific steel grooved plates which are tied through high-strength bolts and disc springs. By slipping of grooved plates, the input energy is dissipated through frictional resistance. Based on the free body diagrams presented in Fig. 1(c), the design procedure is developed for the prediction of the performance of the RSFJ (Zarnani et al. 2016). The slip force (F_{slip}) and residual force (F_{res}) can be determined by Eq. (1) and Eq. (2), respectively:

$$F_{RSFJ,slip} = 2 * n_b * F_{b,pr} * \left(\frac{\sin\theta + \mu_s * \cos\theta}{\cos\theta - \mu_s * \sin\theta} \right) \tag{1}$$

$$F_{RSFJ,res} = 2 * n_b * F_{b,pr} * \left(\frac{\sin\theta - \mu_k * \cos\theta}{\cos\theta + \mu_k * \sin\theta} \right) \tag{2}$$

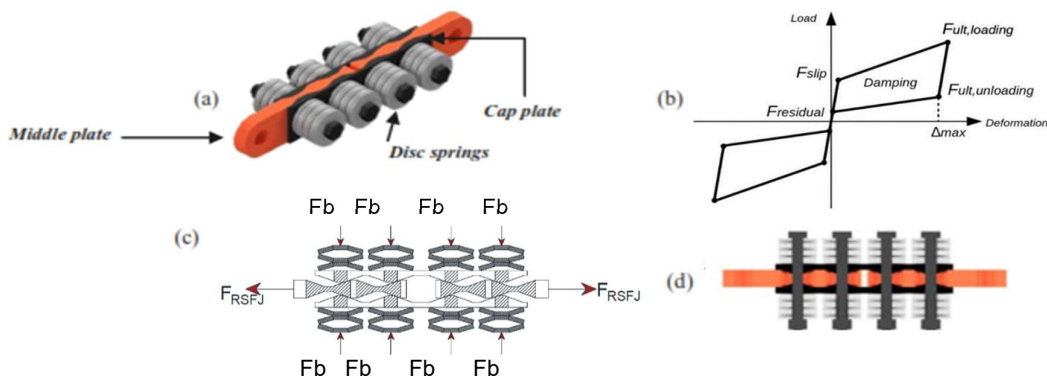


Figure 1. RSFJ device: a) assembly; b) hysteresis; c) free body diagram; d) the joint at rest

Where n_b =number of bolts on each splice, θ =groove angle, $F_{b,pr}$ is the clamping force of prestressing and the μ_s and μ_k are the static and kinetic coefficient of friction respectively, while considered $\mu_k=0.85\mu_s$ (Hashemi et al. 2017). The general hysteresis behaviour of RSFJ is illustrated in Fig. 1(b). $F_{ult,loading}$ and $F_{ult,unloading}$ are the system forces at the maximum disc springs displacement and bolts force.

$$F_{b,u} = F_{b,pr} + K_s * \Delta_s \tag{3}$$

$F_{ult,loading}$ and $F_{ult,unloading}$ is derived by replacing the bolt forces in Eq. 1 and Eq. 2 by Eq. 3, and μ_s , μ_k with μ_k , μ_s .

The Proposed Analysis and Design Procedure

The structural analysis and design procedure for the building using RSFJ as the damping system is developed based on the basic equation presented in previous section. The main objective of the procedure is to obtain an appropriate equivalent ductility factor and determine an efficient size of damping devices. Overall, the procedure is initiated by assuming an initial equivalent ductility factor which is then followed by calculating the seismic demand and determining the size of RSFJ devices. Then, the proposed numerical model of the building structure is verified using the Nonlinear Pushover Analysis (NPA) and Nonlinear Time History Analysis (NTHA). In this procedure, the Force-Based Design (FBD) method is used to estimate estimate the force demand for both loading states, serviceability limit state (SLS), and ultimate limit state (ULS). Furthermore, the Equivalent Static Method (ESM) is used to calculate the seismic demand of the building structure. The detail procedure is presented in Figure 3.

The Design of the Case Study Building

An eight-storey reinforced concrete building structure with a concrete coupled wall as its seismic resisting system is proposed in this research project to evaluate the proposed analysis and design procedure. The concrete coupled walls are used in the middle of the building to minimise the torsional effects. Meanwhile, the RSFJs are used as the hold-down at the bottom corner of the wall and as the shear link in the middle of the coupling beam. To satisfy the requirement of NZS1170.5: 2004, the following criterion is set for the design philosophy: (a) the Ultimate Limit State (ULS) lateral drifts are kept under 1.4 % to minimize the damage to structural and non-structural components (b) the structure remains elastic, the dampers are not activated and the lateral drift ratios are kept 1.5 % and 0.33 % for Ultimate Limit State (ULS) and Serviceability Limit State (SLS) cases, respectively (c) the structure has zero or negligible residual displacement at the end of the seismic event.

The building plan is 35 m by 35 m and is symmetrical about the two main axes. Along each axis, a concrete coupled wall equipped with RSFJ is used as the Lateral Load Resisting System (LLRS). A novel type of shear key is installed at the wall's base to provide displacement compatibility and transfer the shear forces from the wall to the foundation (Hashemi and Quenneville, 2017). The total building height is 28 m and has an identical storey height of 3.5 m. The building is designed for office application (i.e. importance level 3), is located in Christchurch, and is built on the soft soil layer (i.e. soil class type D). Figure 2. illustrates the developed model used in this research project.

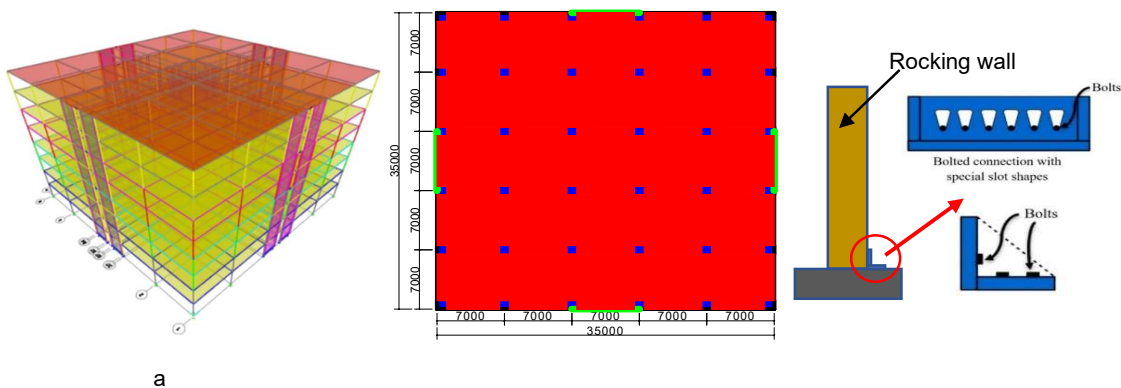


Figure 2. The proposed model: (a) 3D Model; (b) plan view; (c) novel shear key

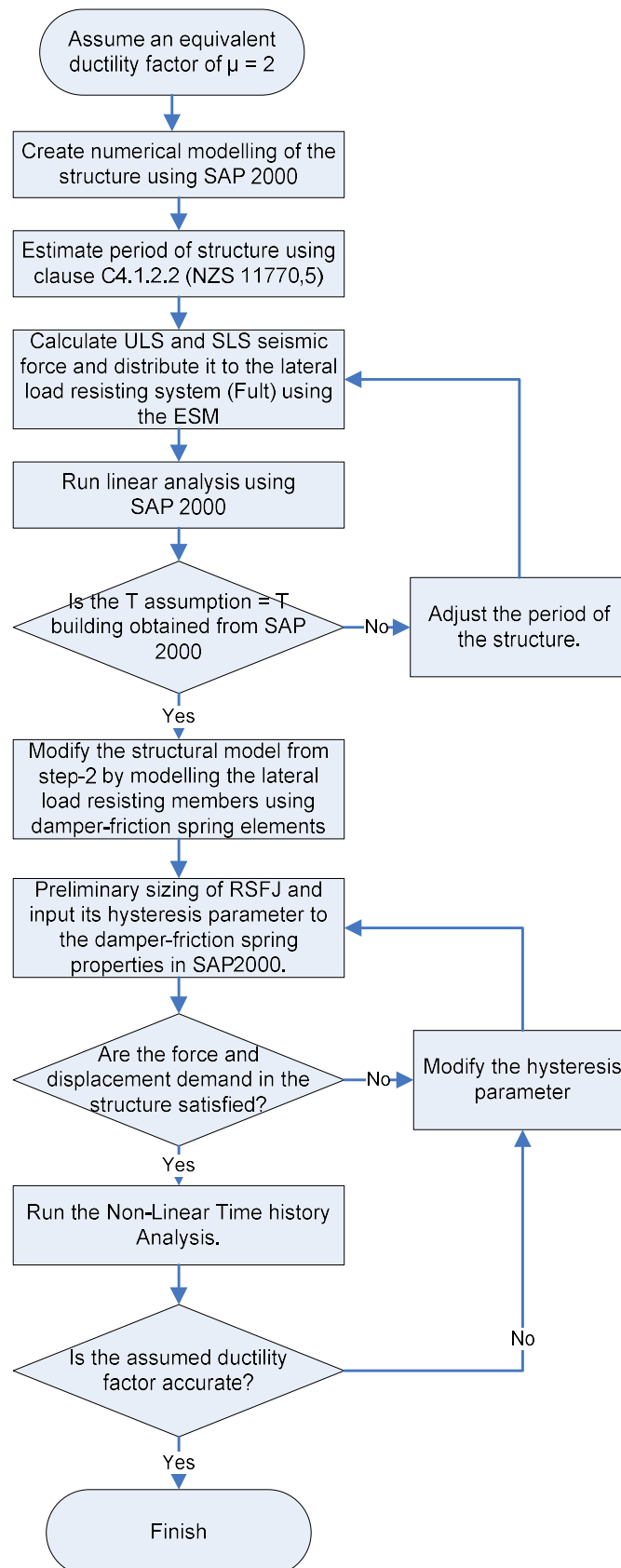


Figure 3. The Proposed Analysis and Design Procedure

The above procedure in Figure 3 can be described in more detailed step by step as follows:

1. Assume an initial equivalent ductility of 2.
2. Create numerical modelling of the structure using SAP 2000 as described in the previous section. Please note that there is no need to model the flag-shaped hysteresis of the RSFJ damping system at this stage.
3. Estimate the initial fundamental period of structure using empirical formula as follow:

$$T_1 = 1.0 * k_t * h_n^{0.75} \text{ (for SLS)} \quad (4)$$

and

$$T_1 = 1.25 * k_t * h_n^{0.75} \text{ (for ULS)} \quad (5)$$

where:

$$k_t = 0.075$$

h_n = the total building height

The fundamental period (T_1) obtained from Eq. 1 and Eq. 2 is 0.913 second and 1.14 second for SLS and ULS case, respectively.

Note that the assumed equivalent ductility factor in this step is the designer's first assumption. The procedure is designed to verify this assumption and the ultimate goal is that the RSFJs are sized appropriately, and the system satisfies the ductility requirement. The structural performance factor (S_p) is considered as 0.7. Note that the P-Delta effect is not considered for this example but for a more detailed design in real cases, it must properly be considered.

4. Calculate ULS and SLS seismic force and distribute it to the lateral load resisting system (F_{ult}) using the Equivalent Static Method.
5. Run the linear analysis using SAP 2000.
6. Check if the initial assumption of structure period is equivalent to structure period obtained from SAP 2000 structural analysis or not.
7. The period of the structure (T_1) at this stage is determined as 0.95 second (SLS) and 1.2 second (ULS) from the modal analysis which is higher than what was assumed in step 3. Therefore, the steps 3 should be repeated with this new value. Following the ESM with the new period, the base shear of the structure is reduced from 17818.1 kN to 14,841 kN.
8. Modify the structural model in SAP2000 and use non-linear elements to represent RSFJs. The "Damper-Friction-Spring" can be used for the shear link and the hold-down, while the "Gap" element can represent the rocking foundation at the wall's toe. At this stage, an elastic drift of 0.2% is assumed for the RSFJ system. The hysteresis parameter for the RSFJ can be estimated using formula as follows:

$$F_{ult} = \text{Base shear of ULS case} \quad (6)$$

$$F_{slip} = \text{Base shear of SLS case} \quad (7)$$

$$F_{restore} = 0.4 * F_{ult} \quad (9)$$

$$F_{residual} = 0.15 * F_{ult} \quad (10)$$

9. Run the non-linear static push-over analysis to obtain the force (i.e., the target drift and the base shear). The hysteresis curve obtained from non-linear pushover analysis is shown in Figure 4. It should be noted that the hysteresis curve presented at this stage is obtained from the first iteration. It is evident that the maximum force and the target lateral drift in the developed model is 14,749 kN and 419 mm which are consistent with the estimated base shear obtained by ESM formula (i.e., 14,841 kN). To ensure that the structural system is well conditioned and behave appropriately, the observation on rotation of the structural element and connection is essential to be carried out.

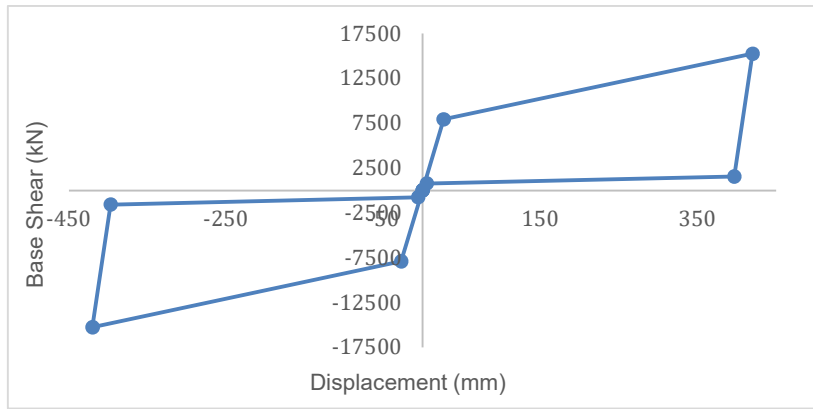


Figure 4. The hysteresis curve from pushover analysis on the first iteration

10. Evaluate whether the target drift and the base shear are consistent with that generated from the ESM formula. Perform iteration until these parameters satisfy the requirement.
11. Run the non-linear time history analysis (NLTHA) to validate the base shear and the equivalent ductility factor (μ). The analysis result of the NLTHA obtained from the first iteration is presented in Figure 5.

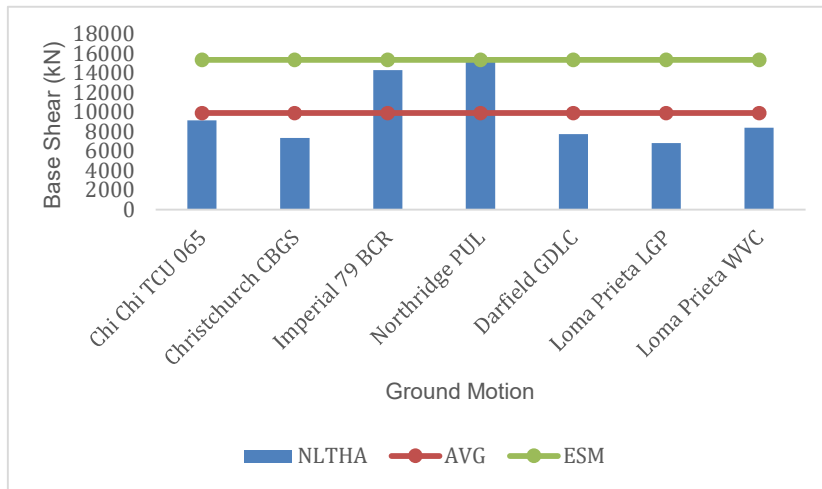


Figure 5(a). The base shear obtained from NLTHA using $\mu = 2$

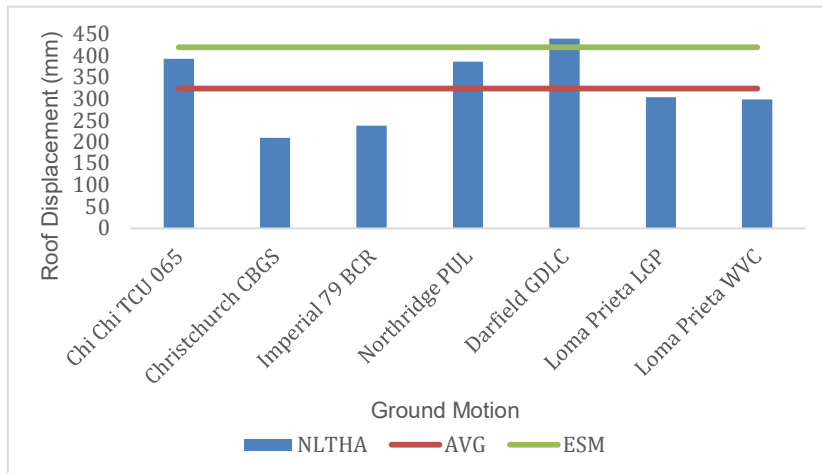


Figure 5(b). The roof displacement obtained from NLTHA using $\mu = 2$

It can be seen from Figure 5. that the average base shear and roof displacement obtained from NLTHA is 9912 kN and 1.06% respectively, which is significantly lower than that estimated using the ESM formula. Therefore, the process should be iterated using a higher equivalent ductility factor (μ) to satisfy the relevant requirements.

12. Following the fourth iteration, the new fundamental period of 1.3 second and the new ductility factor of 2.9 are obtained. Given that these parameters are considerably higher than the initial parameters (i.e., the fundamental period of 1.21 second and the ductility factor of 2.0), the procedure need to be iterated with the new parameters. The spectral shape factor ($Ch(T)$) need to be modified according to NZS 1170.5. Meanwhile, the hazard factor (Z), the return period (R), the near-factor (N), and the structural performance factor (S_p) is remain the same with the initial calculation.
13. According to flowchart in Figure 3, the key parameters of the RSFJs need to be re-determined.
14. Iterate the nonlinear static pushover analysis to investigate the nonlinear behaviour of the structure. Figure 5 shows the new hysteresis curve from the fourth iteration.
15. It can be seen from Figure 5 that maximum base shear is 9987 kN and the target roof displacement is 419 mm which satisfy the demands (i.e., 10,235 kN and 420mm).
16. Run the NLTHA to verify the base shear and the new equivalent ductility factor (μ). The analysis result of the NLTHA obtained from the fourth iteration is presented in Figure 6. Please note that the discussion of the above analysis result is presented in the next section.

RESULTS AND DISCUSSION

The Nonlinear Pushover Analysis

The base shear generated from pushover analysis is 9.99×10^5 kg, which is slightly lower than that of the ESM calculation (1.0235×10^6 kg). Meanwhile, the lateral drift from pushover analysis is 1.5 % (i.e. 420 mm), which satisfies the target displacement. Moreover, the flag-shaped hysteresis curve, which is the main characteristic of the self-centring system can be reasonably achieved. It is observed from the hysteresis curve that the structure remains elastic up to 0.2 %. After this point, the RSFJs start to activate, resulting in the observed bi-linear pushover curve. It should be noted that since not all RSFJs are activated at the same time, a transition zone from the linear elastic zone to the geometrically nonlinear zone is observable in the pushover curve. Nevertheless, the entire structure remains elastic, and no material nonlinearity is expected within the transition zone. Figure 6. depicts the final hysteresis curve obtained from pushover analysis for the proposed structural system.

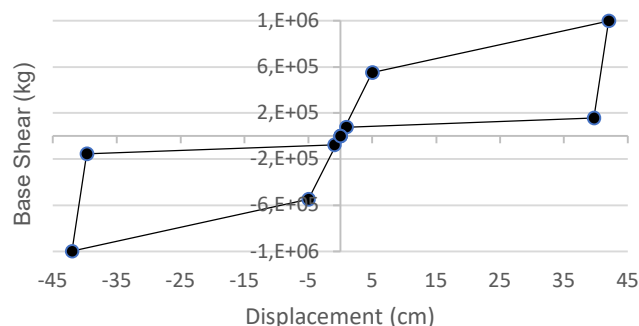


Figure 6. The final hysteresis curve obtained from non-linear pushover analysis

Nonlinear Dynamic Time-History Simulations

The NLTHA results are about 4 % lower than that calculated with the ESM. In this study, the average of seven ground motions is considered for analysis and an equivalent ductility factor of $\mu=2.9$ is used for the developed model. Figure 7. illustrates the base shear and roof displacement obtained from NLTHA. NLTHA H1 and NLTHA H2 refers to analysis for x-axis and y-axis, respectively.

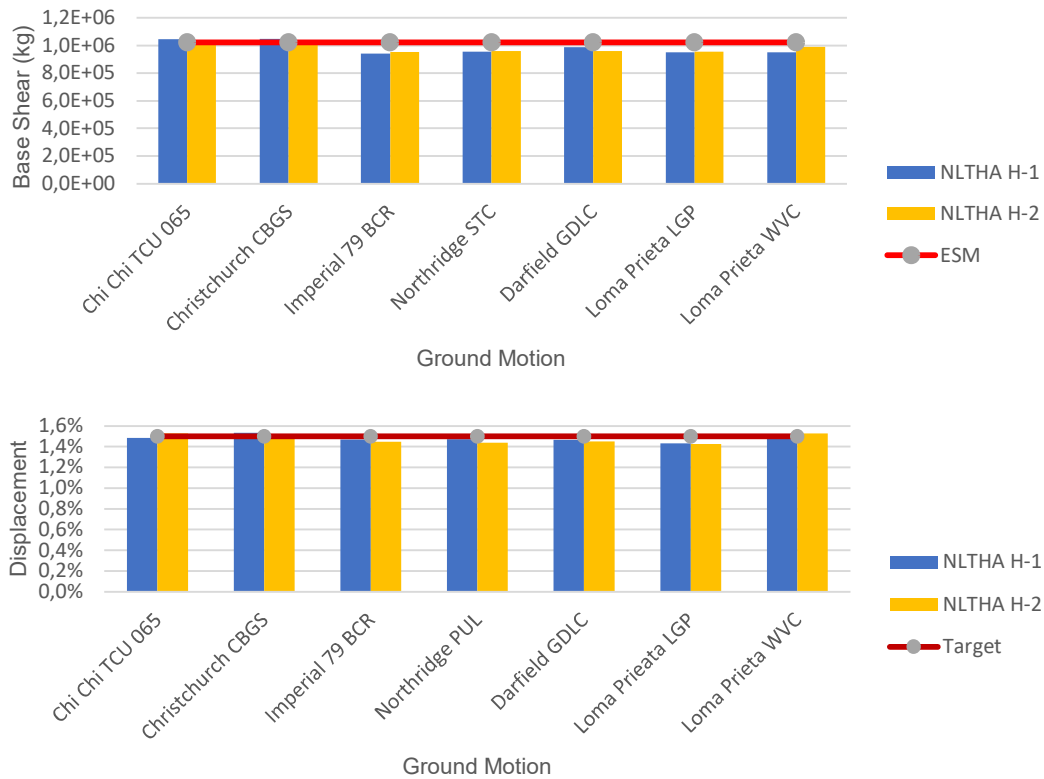


Figure 7. NLTHA Result: (a) base shear comparison; (b) roof displacement comparison

The chart shows that the highest base shear is obtained from the Christchurch CBGS and Chi-Chi TCU event which are accounted at 1.048×10^6 kg and 1.045×10^6 kg, re-spectively. Similarly, the highest roof displacement is generated from the Christchurch and Chi-Chi TCU event, which are recorded at 43.1 cm and 42.6 cm. The average base shear is accounted for at 9.824×10^5 kg, which is slightly lower than that of the ESM estimation (10.235×10^5 kg). Meanwhile, the average roof displacement is calculated at 1.46%, which is 0.04% lower than the target drift (i.e. 1.5%). If the mean of the recorded drifts is taken, it reasonably satisfies the target drift and confirms the predicted seismic performance of the developed structural model.

Inter-Storey Drift

It can be seen in from Figure 8. that the maximum inter-storey drift of the proposed model is about 1.5%, which is significantly lower than the requirement in the NZS 1170.5.

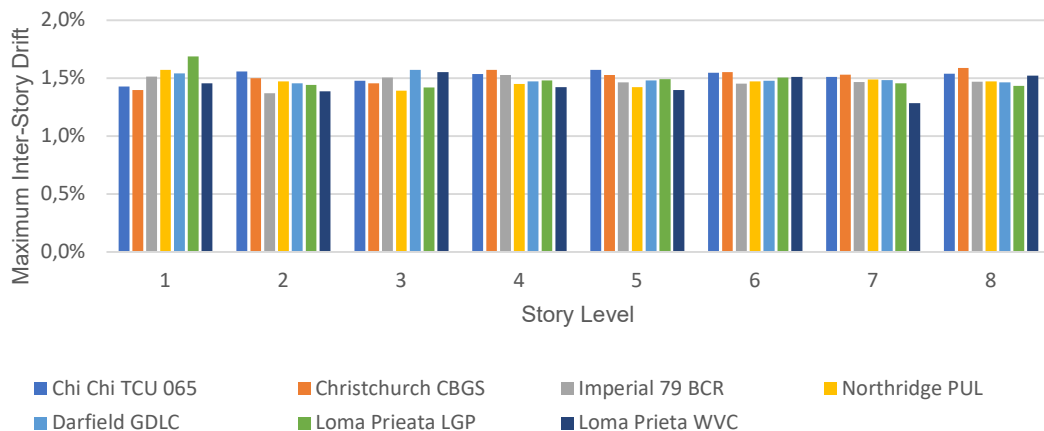


Figure 8. NLTHA Result: Inter-storey drift

It means that the configuration of the RSFJ and the lateral resisting system can prevent the “soft storey” formed at any building level. The highest and the lowest inter-storey drift is recorded for the Loma Prieta LGP (1.61 %) and the Imperial 79 BCR (1.37 %), respectively. These values are well close to the target lateral drift, which shows the accuracy of the proposed design and analysis method.

The Residual Drift

To achieve the full self-centring behaviour, the maximum residual drift at the end of NLTHA shall be limited at 0.2% and 0.25% for the design level intensity earthquake and for the maximum considered earthquake (MCE) intensity, respectively (Henry et al., 2011). Figure 9 shows the residual drift from Chi-Chi and Christchurch event which is less than 8mm (i.e., less than 0.2%). The residual drift from other events is less than 6mm. Therefore, these residual drifts will result in the negligible structural damage and minor cosmetic repairs after earthquake. It confirms the fully self-centring behaviour (i.e., with-out relying on any supplementary devices such as the post-tensioned strands), which can be attributed to the RSFJs used in the LLRS.

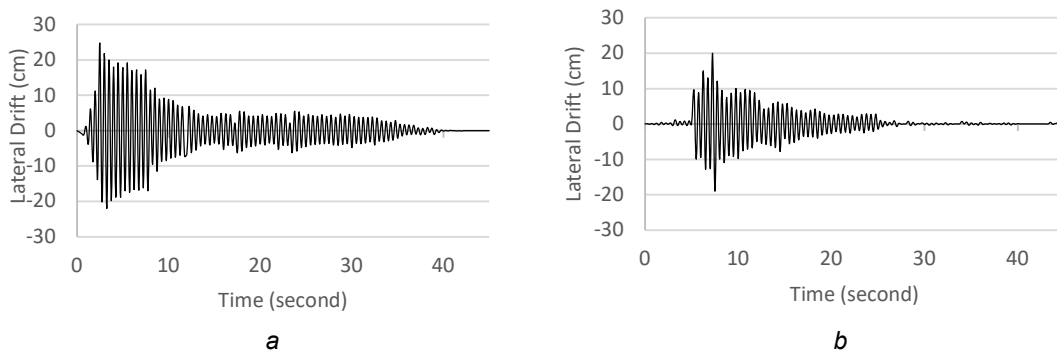


Figure 9. Residual drift: (a) Chi-Chi event; (b) Christchurch event

Response Of the Individual RSFJ

Overall, each RSFJ performs within its capacity and achieve its desired lateral displacement. According to the analysis results, the internal forces (i.e. shear force for the shear links and axial force for the hold-downs) are lower than their ultimate force ($F_{ult,loading}$). Furthermore, these individual responses of the RSFJs show the efficiency of the proposed structural wall system and design procedure in controlling lateral drift.

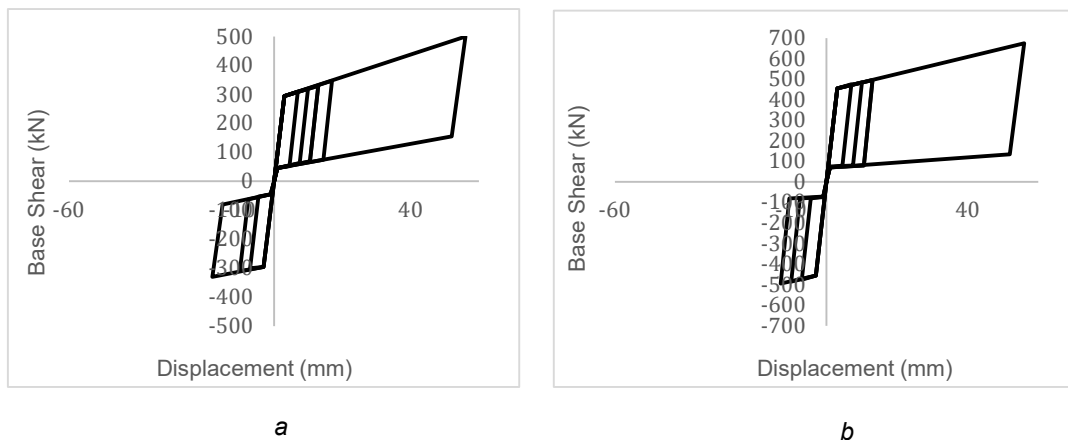


Figure 10. Response of individual RSFJ: (a) Hysteresis on the First Level; (b) Hysteresis on the Roof Level

Figure 10 describes that the general hysteretic behaviour of the joint is consistent with the results of the quasi-static analysis conducted by Hashemi (2017). The maximum displacements are 15 mm in compression and 55 mm in tension, which the latter is close to the specified displacement for the joint (i.e., 59 mm).

Conclusion

This paper provides a step-by-step analysis and design procedure for structures that use RSFJs in their lateral resisting systems. In this paper, the application of self-centring friction damping on the eight-storey building structure is proposed and its performance is analytically and numerically observed. This innovative RSFJ system is incorporated in a coupled concrete wall system with the aim of achieving damage avoidance. In the developed model, the RSFJs are employed as the shear links between the coupling beams and as the hold-down in the wall's toe. The following conclusion is observed after the NTHA of the structural system:

1. The developed structural model can produce an ideal flag-shaped hysteresis curve, which is a key feature for a low damage design structure. It means that the damping devices employed in the structure do not only have a good energy absorption but also an excellent self-centring behaviour. Therefore, the proposed prototype can be considered as an efficient alternative to traditionally high-damage lateral resisting systems to minimise and localise damages. In this way, the life-safety and immediate occupancy criteria can be achieved.
2. The proposed RSFJs configuration can achieve an equivalent ductility factor of μ equal to 2.9, which is significantly higher than the ductility coefficient for the conventional structures (i.e., $\mu=2$). It means that the application of RSFJs in the lateral resisting system results in a more economical design than the conventional structural design.
3. The proposed equations developed in the previous section can easily calibrate the key parameters of the RSFJs and produce the flag-shaped hysteresis curve. By using this equation, a low number of iterations are required to generate an equivalent ductility factor for the seismic resilient structure with RSFJs. In this paper, an initial equivalent ductility factor (μ) of 2 is adopted at the start of the design because the ultimate force ($F_{ult_loading}$) is defined from the base shear at ULS case (with $\mu=2$). In this way, it requires only four iterations to obtain the optimum equivalent ductility factor.

ACKNOWLEDGEMENT

The authors would like to thank Ministry of Foreign Affairs and Trade of New Zealand (MFAT) for the financial support of this research.

REFERENCES

- Aslam, M., Godde, W. G., & Scalise, D. T. (1978). Earthquake rocking response of rigid bodies. University of California, Berkeley. <https://escholarship.org/uc/item/07b7w0rv>
- Darani, F. M., Zarnani, P., Hashemi, A., Bagheri, H., Quenneville, P., & Hammerle, E. (2019). Self-centring pre-cast concrete shear walls with resilient slip-friction joints: a new seismic damage avoidance structural system. Fifth Conference on Smart Monitoring, Assessment and Rehabilitation of Civil Structures.
- Hashemi, A. (2017). Seismic resilient multi-story timber structures with passive damping. University of Auckland, New Zealand
- Henry, R. S., Sritharan, S., & Ingham, J. M. (2011). Recentring requirements for the seismic design of self-centring systems. the Ninth Pacific Conference on Earthquake Engineering Building an Earthquake-Resilient Society, Auckland, New Zealand.
- Housner, G. W. (1963). The behaviour of inverted pendulum structures during earthquakes. Bulletin of the Seismological Society of America, 53(2). 403-417.
- NZS 1170.5:2004 (2004). Structural design action part 5: Earthquake actions. New Zealand Standard Executives. <https://www.standards.govt.nz/>
- NZS 3101.1:2006 (2006). Concrete Structure Standard part 1: The design of concrete structures. New Zealand Standard Executives. <https://www.standards.govt.nz/>
- Priestley, M.J.N., Sritharan, S., Conley, J.R. & Pampanin, S. (1999). Preliminary results and conclusions from the PRESSS five-story precast concrete test building. PCI Journal, 44(6), 42-67.
- Sahami, K., Veismoradi, S., Zarnani, P., & Quenneville, P. (2019, April 4-6). Seismic performance of rocking concrete shear walls with Innovative Rotational Resilient Slip Friction Joints. 2019 Pacific Conference on Earthquake Engineering and Annual NZSEE Conference.